Physica Scripta

PAPER

Optoelectronic and thermoelectric characteristics of lead-free halide based double perovskites Rb_2GaInX_6 (X = Cl, Br, I) for solar cell applications

To cite this article: Ayesha Ejaz *et al* 2022 *Phys. Scr.* **97** 115704

Physica Scripta

PAPER

Optoelectronic and thermoelectric characteristics of lead-free halide based double perovskites Rb_2GaInX_6 (X = Cl, Br, I) for solar cell applications

RECEIVED
27 July 2022

REVISED
13 September 2022

ACCEPTED FOR PUBLICATION
13 October 2022

PUBLISHED
26 October 2022

Ayesha Ejaz[1], **Ghulam M Mustafa**[1,2,*], **Muhammad Amin**[1], **N A Noor**[3,*], **Hamid Ullah**[3] and **R Neffati**[4]

[1] Department of Physics, The University of Lahore, Lahore,53700, Pakistan
[2] Department of Physics, Division of Science and Technology, University of Education Lahore, Pakistan
[3] Department of Physics, RIPHAH International University, Lahore Campus, Pakistan
[4] Department of Physics - Faculty of Science - King Khalid University, PO Box 9004, Abha, Saudi Arabia
[*] Authors to whom any correspondence should be addressed.

E-mail: gmmustafa25@gmail.com **and** Naveed.noor@riphah.edu.pk

Keywords: first-principles study, boltztrap code, mBJ potential, optoelectronic properties, figure of merit, power factor

Abstract

For the fabrication of thermoelectric and optoelectronic devices, metal halide perovskite materials are perfect applicants. In this work, first-principles computation is carried out to explore the structural, optical, electronic, and transport features of Rb_2InGaX_6(X = Cl, Br, I).In structural calculations, the obtained value of Paugh's ratio(B/G) reveals the material's brittleness. The acquired negative value of enthalpy of formation (ΔH_f) exposes the studied materials are stable. The exploitation of band structure exhibits that the Rb_2InGaX_6(X = Cl, Br) compound possesses an indirect bandgap value of 2.20eV for Cl, which significantly decreases to 0.90 eV by substituting anion from Cl up to I. The materials under observation possess a remarkable absorption coefficient $\alpha(\omega)$ in ultraviolet and visible region (2–8eV) of light spectra, which makes it practical for photocell and optical device fabrication. Furthermore, the transport features are estimated by utilizing the BoltzTrap code within the temperature range of 200–500 K. The calculated value of the figure of merit (ZT) indicates that Rb_2GaInX_6 (X = Cl, Br, I) compounds are a potential candidate for thermoelectric device applications.

1. Introduction

Over the past few years, perovskite materials have developed material science and solid-state physics based on their fundamental features. As we live in the era of the environmental energy crisis, with the increasing energy demand, fossil fuels are declining day by day. So, to minimize their depletion, scientists are concentrating on the fabrication of light-harvesting devices that could convert light energy into electrical energy without polluting the environment [1]. Solar energy takes a fractional part in replacing non-renewable sources of energy such as fossil fuels. Spotting the potential material for energy harvesting applications is essential [2, 3]. Earlier lead-based perovskite materials were used to convert light energy into electricity due to their high efficiency of energy conversion, but their toxic nature assists the researchers for an alternative substance. They have found captivated recognition of the organic/inorganic halide-based perovskite in theoretical and experimental consideration since these materials come up with a cheap processing cost, recycling, non-toxic nature, adjustable bandgap, and high-temperature stability, which make them suitable for the fabrication of solar cells power generation devices [4].

Perovskite was the first man who specified the structure of perovskite material. If the unit cell is doubled, they become double perovskites. Their general formula is $A_2BB'O_6$ [5]. These perovskite compounds have promising applications in different fields of sciences. In recent decades, lead-based perovskite materials have become essential in optoelectronic devices. They bring up a massive increase in the power conversion efficiency

greater than 25% through unique fabricating procedures [6]. Due to their toxicity and instability, these materials are prohibited from being used commercially. This has stimulated the researchers to develop lead-free, environmentally friendly materials, high-temperature stability, and cheap processing cost. A noticeable advancement is being made to discover possible applications (such as thermoelectric, optoelectronic, and spintronic) of the lead-free perovskites [5].

In recent years, much work has been allotted to double perovskite materials to investigate their properties for possible applications. Parrey*et al* (2018) find out that the La_2NbMnO_6 compound is half-metallic, and its bandgap energy is 3.75 eV. Furthermore, he found this material suitable for optoelectronic devices in IR and UV frequency ranges. He also predicted the figure of merit as 0.14 [7]. Ullah *et al* (2020) showed perfectly suitable for optoelectronic devices. He also calculated values of optical properties, which show that these perovskites are perfectly suitable for optoelectronic devices [8], Nabi *et al* (2019), used the density functional theory (DFT) to understand how pressure affect the electronic, structural, thermodynamic, and thermoelectric properties of Ba_2MnTaO_6 double perovskites. He showed that compounds have a wide bandgap ranging from 2.63 to 2.56 eV. He calculated the value of the Seebeck coefficient, which is 99.69.[9], Razzaq and Islam (2020) showed that Paugh's ductility index (B/G) talks about the brittleness of the material. The Calculated value of the Zener anisotropic factor supported the anisotropic nature of the compound. The Direct bandgap of this compound is 1.33eV. The compound's semiconducting nature was calculated by the density of states (DOS) and electronic band structures. Cs_2SnBr_6 [10], Dar, S.A. *et al* (2019) investigated the electronic features by computing the different optical parameters that showed the semiconducting nature [11].

In the light of a comprehensive literature review, it is noticeable that the calculated values of the bandgap, absorption coefficient, thermoelectric properties such as Seebeck coefficient, the figure of merit confirm that these materials are suitable for solar cell and thermoelectric device fabrications.

2. Computational methods

To examine the structure, thermoelectric and optoelectronic features of Rb_2InGaX_6(X = Cl, Br) double perovskite, theoretical computations are carried out by implementing the FPLAPW method in WIEN2K software [12]. The modified Becke-Johnson exchange-correlation functions are used within generalized gradient approximation (GGA) to estimate the least total energy value. The value of the tolerance factor (t_G) determines the stability of the compound, and it can be found by using the relation [13]:

$$t_G = \frac{r_A + r_x}{\sqrt{2}\,(r_{BB'} + r_x)} \tag{1}$$

Here r_A, r_B, r_X the ionic radii of respective atoms and this formula determine the stability of crystal strucutre by taking into account the ionic radii of involving atoms. The computed electronic features show the semiconducting nature of the compound. The electronic strucutre calculation was carried out using PBEsol approximation. In addition, the lattice parameter was calculated from the energy volume optimization graph. The unit cell is split up into interstitial region and muffin tin radii R_{MT}. Muffin tin radii are chosen to ensure no charge leakage in the interstitial region and energy convergence [5, 12]. The initial variables have been adapted in the Brillouin zone by Gaussian variables $G_{max} = 16$ and $K_{max} \times R_{MT} = 8$. The wave vector (k) mesh is approximate of 12 × 12 × 12 order chosen by 2000-k upon which energy is liberated. Moreover, optoelectronic features are computed by the Kramer-Kronigformula [11]. The real and imaginary dielectric constants are given as:

$$\varepsilon_1(\omega) = 1 + \frac{2}{\pi} P \int_0^{\infty} \frac{\omega' \varepsilon_2(\omega')}{(\omega')^2 \_ (\omega^2)} d\omega \tag{2}$$

$$\varepsilon_2(\omega) = -\frac{2\omega}{\pi} P \int_0^{\infty} \frac{\varepsilon_1(\omega') - 1}{(\omega')^2 \_ (\omega^2)} d\omega \tag{3}$$

To investigate transport properties of material BoltzTrap code is used that is established on Semiclassical Boltzmann transport theory.

Its expressions are as:

$$\sigma_{a\beta}(\alpha, \mu) = \frac{1}{\Omega} \int \sigma_{a\beta}(\varepsilon) \left[-\frac{\partial f0(T, \varepsilon, \mu)}{\partial \varepsilon} \right] d\varepsilon \tag{4}$$

$$k^{e}_{a\beta\,(T,\mu)} = \frac{1}{e^2 T \Omega} \int \sigma_{a\beta}(\varepsilon)(\varepsilon - \mu) \left[-\frac{\partial f0(T, \varepsilon, \mu)}{\partial \mu} \right] d \tag{5}$$

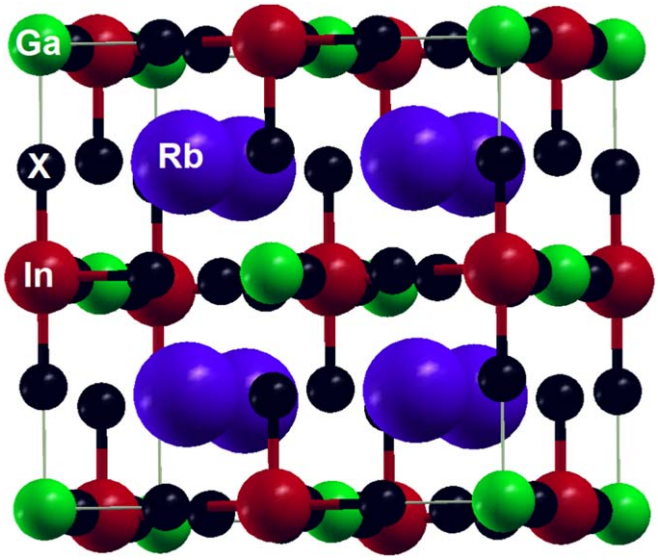

Figure 1. The Cubic structure of double perovskites Rb_2GaInX_6 (X = Cl, Br, I), where the blue, red, green, and black spheres represent Rb, In, Ga, and X atoms.

$$S_{\alpha\beta(T,\mu)}\frac{1}{eT\Omega\sigma_{a\beta}(T,\ \mu)}\int\sigma_{a\beta}(\varepsilon)(\varepsilon\ -\ \mu)\left[-\frac{\partial f0(T,\ \varepsilon,\ \mu)}{\partial\varepsilon}\right]d\varepsilon \tag{6}$$

Here, f_0 is the Fermi–Dirac equilibrium distribution function, Ω shows the volume of crystal structure, and μ is the chemical potential [14].

3. Results and discussion

3.1. Structural properties

Figure1 shows the cubic structure of Rb_2GaInX_6(X = Cl, Br, I) material. The calculated value of lattice parameter (a_o) are noticed as 10.66Å, 11.13Å, and 11.87Å, for Cl, Br, and I-based compositions, respectively. This increase in lattice parameters is credited to the greater ionic size of proceeding halides. The space group can represent the arrangement of atoms in the crystal structure $\overline{Fm3}$ m with their unique Wyckoff positions. The Rb ions sit at the 8c site with atomic coordinates(1/4,1/4,1/4), Ga ions sit at the 4*a* site with coordinates (0,0,0). Similarly, it occupies the 4b site with coordinates (1/2,0,0) while halides take the 24e site with coordinates (x,0,0).

To get a stable energy state at the lowest energy, one must optimize the volume. The volume optimization was done to acquire the lattice constants using the Murnaghan equation [15].

$$P(V) = \frac{k}{k'_0}\left[\left(\frac{v}{v_0}\right)^{k'_0} - 1\right] \tag{7}$$

The volume energy graph for all three compositions is shown in figure 2. Table 1 comprises the computed values of lattice parameters. Based on this data, one can predict that the computed parameters agree with the reported experimental values [16–17].

3.2. Phonon spectra

The phonon dispersion spectra of Rb_2GaInX_6 (X = Cl, Br, I) double perovskites were computed using PBEsol functional of TB-mBJ potential and are presented in figure 3. In these compositions, there are 10 atoms and thus 30 phonon modes which are divided in two main types called acoustic and optical phonons. Optical phonons have a greater wavelength at a lower frequency. The positive value of frequency in the complete BZ assured the stability of under study compositions of double perovskites [18].

3.3. Mechanical properties

The material is mechanically stable if it satisfies the necessary condition of stability known as Born stability criteria, i.e., $C_{11} > 0, C_{44} > 0, C_{11}–C_{12} > 0$, and $C_{11} + 2C_{12} > 0$, where $C_{11}, C_{12}, C_{44}$are elastic constants [10]. The computed values of the Bulk modulus(B) and Shear modulus (G) are also given below in table 1, which shows that

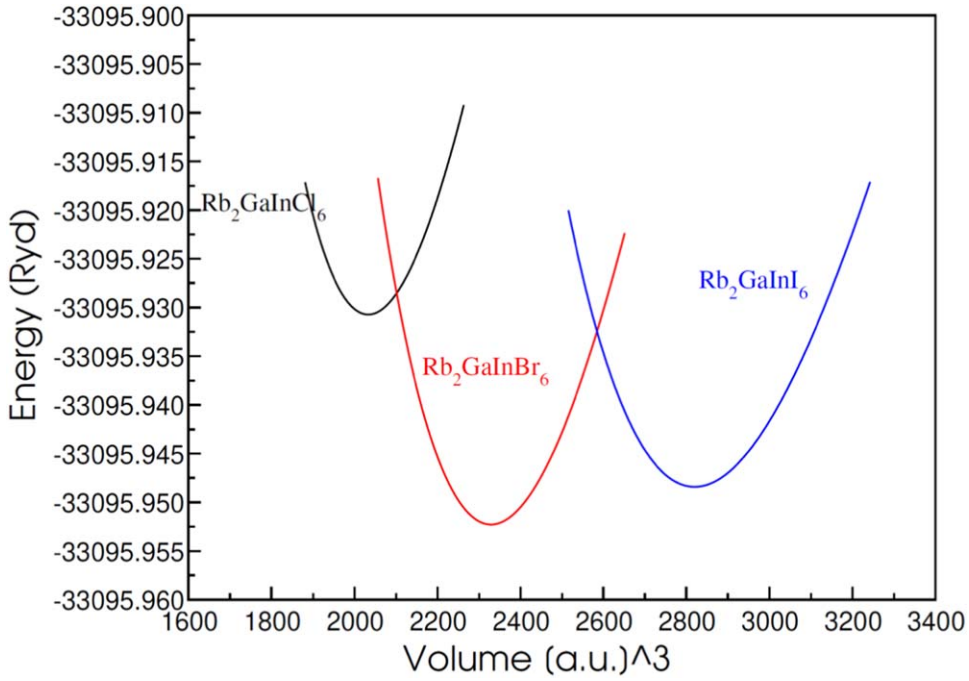

Figure 2. Volume versus energy graph of studied compound Rb_2GaInX_6 (X = Cl, Br, I).

Table 1. The calculated values of structural and mechanical parameters of Rb_2GaInX_6 (X = Cl, Br, I).

Structural parameters	$Rb_2GaInCl_6$		$Rb_2GaInBr_6$		Rb_2GaInI_6	
	PBEsol	Other Cal.	PBEsol	Other Cal.	PBEsol	Other Cal.
A_o	10.66	10.82[a]	11.13	11.36[a]	11.87	12.15[a]
B_o	29.11		26.13		20.60	
t_G	0.95		0.96		0.98	
ΔH_f	−1.64		−1.08		−0.82	
C_{11}	54.11		49.67		32.77	
C_{12}	16.92		14.22		13.87	
C_{44}	8.31		7.24		3.75	
B	29.31		26.03		20.17	
G	11.54		10.46		5.48	
Y	30.62		27.67		15.09	
B/G	2.53		2.48		3.68	
υ	0.34		0.33		0.37	
A	0.44		0.40		0.39	

the material is rigid. The value of Pugh ratio B/G shows the ductility/brittleness of the material. The calculated value of Pugh's ratio is more significant than 1.75, which shows that the materials under investigation are ductile [17].

The calculated enthalpy of formation (ΔH_f) is given in Table 1. The enthalpy of formation can determine the thermodynamic firmness. The observed negative values of ΔH_fpredict that heat is released during the formation of the compound, and it is more stable. The calculated values of Young's modulus (Y) and anisotropy factor (A) are also given below.

3.4. Optoelectronic features

The computation of partial density of states, and total density of states provide useful information about optoelectronic features of Rb_2GaInX_6 (X = Cl, Br, I) [19]. The consequences indicates that the three compositions $Rb_2GaInCl_6$, $Rb_2GaInBr_6$, Rb_2GaInI_6 have indirect bandgap values of 2.20 eV, 1.55 eV, 0.90 eV respectively (shown in figure 4). Moreover, in the Brillouin zone, conduction band minima of the compositions are at L, and valence band maxima deceits at X crystallographic position. By changing anion from Cl to I, the width of the bandgap is reduced. The conduction band (CB) moves near the Fermi level (reduction in the bandgap) due to increased atomic size while moving down the group from Cl to I [20].

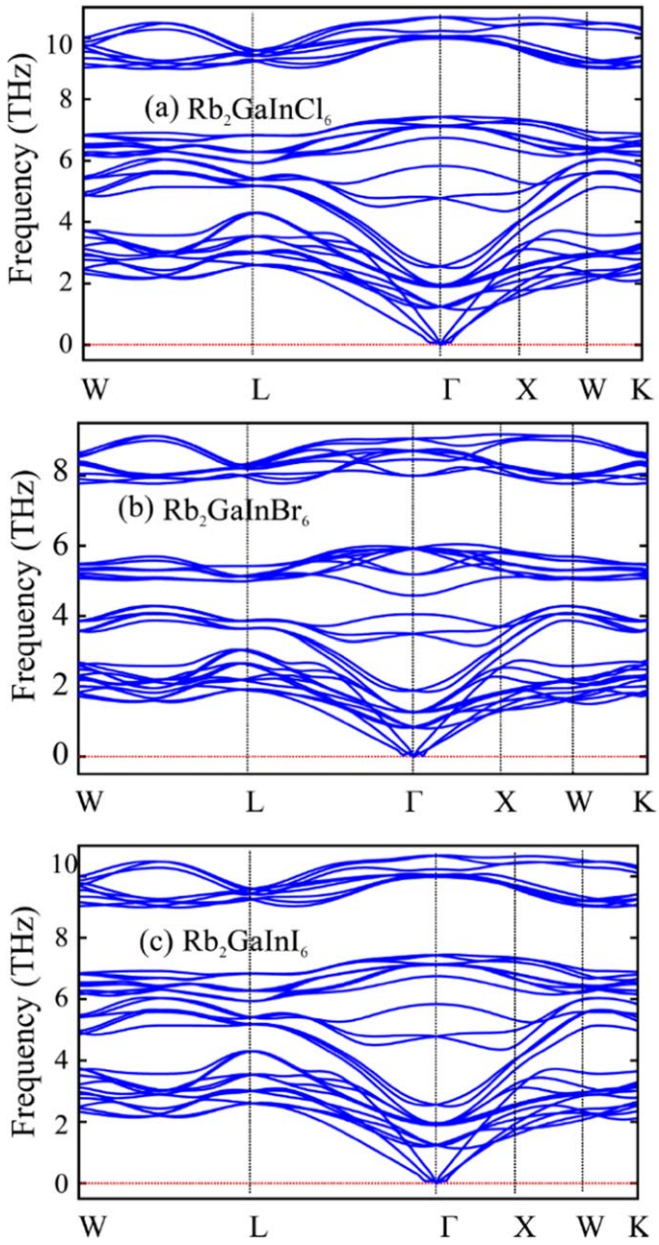

Figure 3. Phonon dispersion spectra of Rb_2GaInX_6 (X = Cl, Br, I).

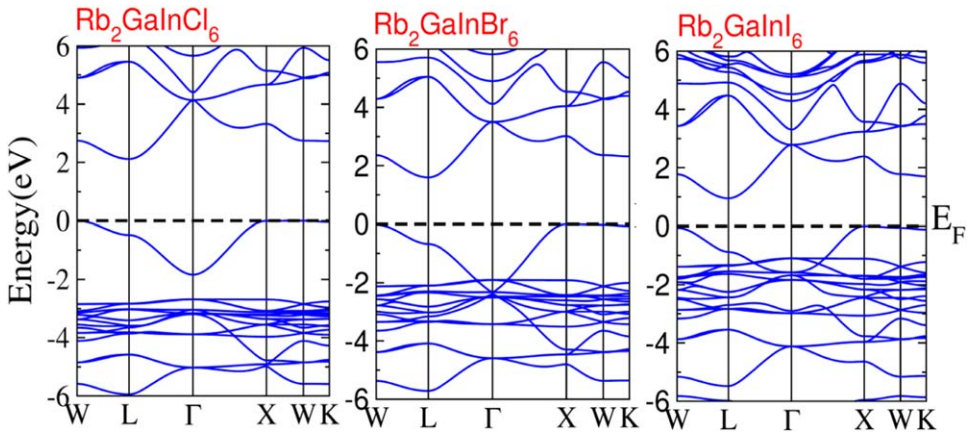

Figure 4. DFT calculated electronic band structures of Rb_2GaInX_6 (X = Cl, Br, I).

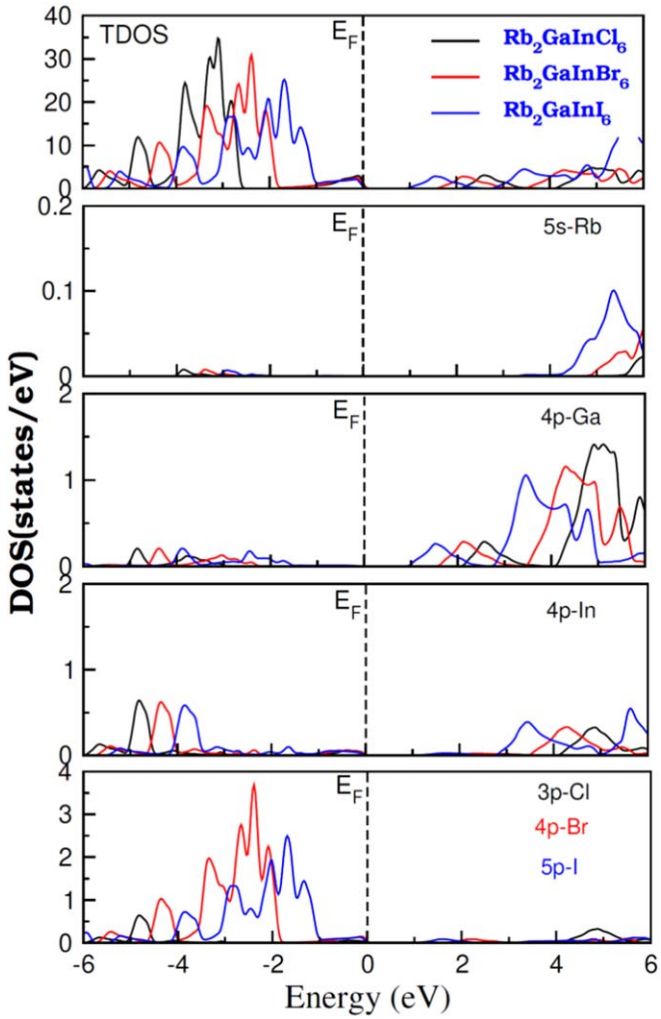

Figure 5. Calculated TDOS of Rb_2GaInX_6 (X = Cl, Br, I) and PDOS of Rb, Ga, In, and X atoms with mBJ potential.

Generally, in the formation of band gaps, the graphs of DOS show the contribution of different states, and total density of states (TDOS) represents the contribution of all the three compositions that are Rb_2GaInX_6 (X = Cl, Br, I). Partial density of states (PDOS) provides a better insight into the contribution of different elements in band formation. It is clear from figure 5 that the *5s* state of Rband *4p* state of Ga plays a vital contribution in forming the conduction band. At the same time,*4p*-In has a minor contribution in band formation both in valence and conduction band. Furthermore, in forming the valence band, halogens have additional feasibility of states *3p/4p/5p* of Cl, Br, and I, respectively.

The interaction of light with matter instigates electrons for interband and intra-band transition. The inter-band transition is appropriate for optoelectronic applications. In addition, the bandgap of the compound is a subsequential parameter since it talks about that particular region where maximum energy absorption takes place. It can be seen from figure 6 that the real part of the dielectric constant corresponds to the refraction, whereas the imaginary part corresponds to the extinction coefficient. The highest peaks show the maximum absorption of light.

The maximum crust obtains due to the resonance of frequency of light with the vibrational frequency of material particles. Different values of optical variables such as refractive index (n), dielectric constant (ε), absorption (α), and reflectivity (R) for the material Rb_2GaInX_6 (X = Cl, Br, I) are displayed in table 2.

The real part of the dielectric parameter $\varepsilon_1(\omega)$ reaches maximum values of 3.29, 3.92, and 5.10 for $Rb_2GaInCl/Br/I_6$, respectively, as shown in figure 6. A rising value in real part of the dielectric constant is noticed while moving from Cl to I, which is 3.29 to 5.10. This increase in value is in accordance with Penn's model [19]. $\varepsilon_1(\omega) \approx 1 + (\hbar^{\infty}\omega_p/E_g)^2$which predicts that the compound is appropriate for optoelectronic device applications. Computed zero energy refractive index $n(\omega)$ are given in table 2, and it can be calculated by the following formula [21]:

$$n(\omega) = [\sqrt{\{\varepsilon_1^2(\omega) + \varepsilon_2^2(\omega) + \varepsilon_1(\omega)\}}]^{1/2} \quad (8)$$

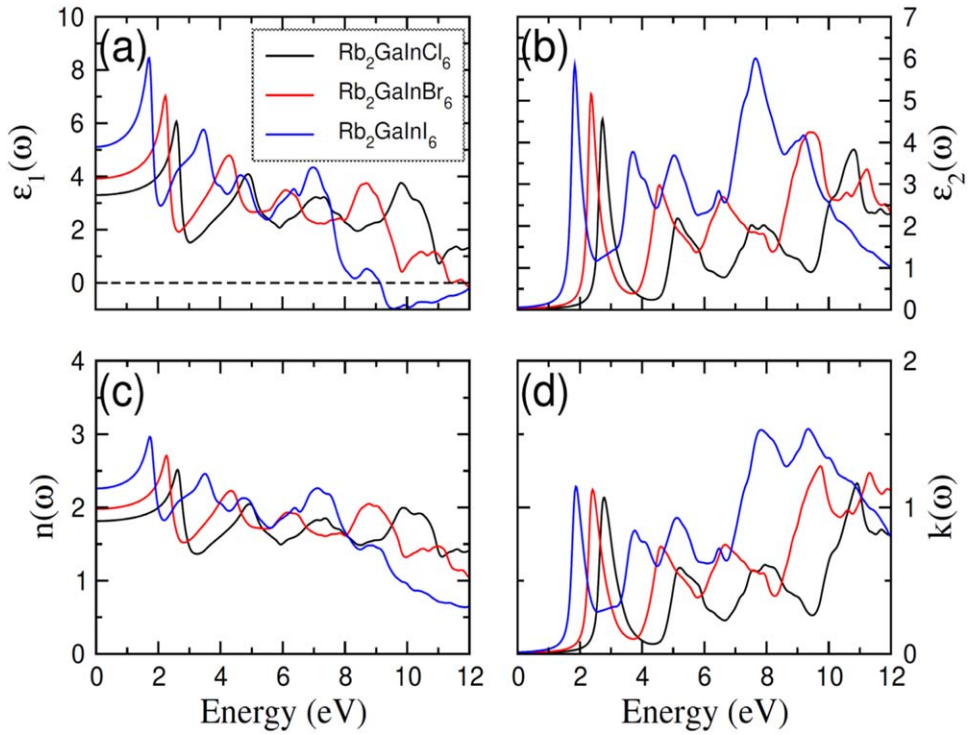

Figure 6. The estimated values of real part $\varepsilon_1(\omega)$, imaginary part of dielectric function $\varepsilon_2(\omega)$, Refraction and coefficient of extinction for Rb_2GaInX_6 (X = Cl, Br, I) by using mBJ-potential.

Table 2. Estimated values of bandgap and optical constants by using mBJ potential at zero for cubic structure Rb_2GaInX_6 (X = Cl, Br, I).

Spinel	E_g(eV)	ε_1	n	R
$Rb_2GaInCl_6$	2.20	3.29	1.81	0.08
$Rb_2GaInBr_6$	1.55	3.92	1.98	0.10
Rb_2GaInI_6	0.90	5.10	2.26	0.15

The absorption parameter $\alpha(\omega)$ controls that up to a point, the wavelength of light could absorb into the material. The highest absorption crest is found in UV and visible regions within the energy range of 2–8eV. At zero energy, the reflectivity (R)value was observed at 0.08 for Cl and 0.15 for I.The variation of $\alpha(\omega)$, $\sigma(\omega)$ and R(ω)within the energy range of 0–12 eV is shown in figure 7.

3.5. Thermoelectric features

To manufacture energy conservation devices that can convert heat to electrical energy, one needs materials with acceptable values of the Seebeck coefficient and figure of merit. The thermoelectric features of Rb_2GaInX_6 (X = Cl, Br, I) are computed by classical Boltzmann transport theory and executed in BoltzTrap code [22]. The figured values of thermoelectric features are given in table 3. A perfect thermoelectrical material should have a high value of electrical conductivity(σ/τ)and Seebeck coefficient (S) and a low value of thermal conductivity(k/τ) [13]. Figure 8 labels the transport properties for Rb_2GaInX_6 (X = Cl, Br, I) material against Temperature (K).

The electrical conductivity of depends upon the carrier concentration, carries mobility and charge on each charge carrier and it is proportional to the number of free charge carriers. The values of σ/τ are 6.51/5.74/2.63 ($\Omega\,ms^{-1}$) for Rb_2GaInX_6 (X = Cl, Br, I) compounds, respectively. It can be noticed from figure 8 that with the gradual increase in temperature, σ/τ also increases. This increase in the value of σ/τ is attributed to the increasing carrier concentration as a result of bond breaking. The mathematical expression of $\sigma_{a\beta}$ is as follows:

$$\sigma_{a\beta}(\alpha,\ \mu) = \frac{1}{\Omega}\int \sigma_{a\beta}(\varepsilon)\left[-\frac{\partial f0(T,\ \varepsilon,\ \mu)}{\partial \varepsilon}\right] \tag{9}$$

wheref_0 represents the Fermi–Dirac equilibrium distribution function, μ is the chemical potential, and Ω shows the volume of crystal structure.

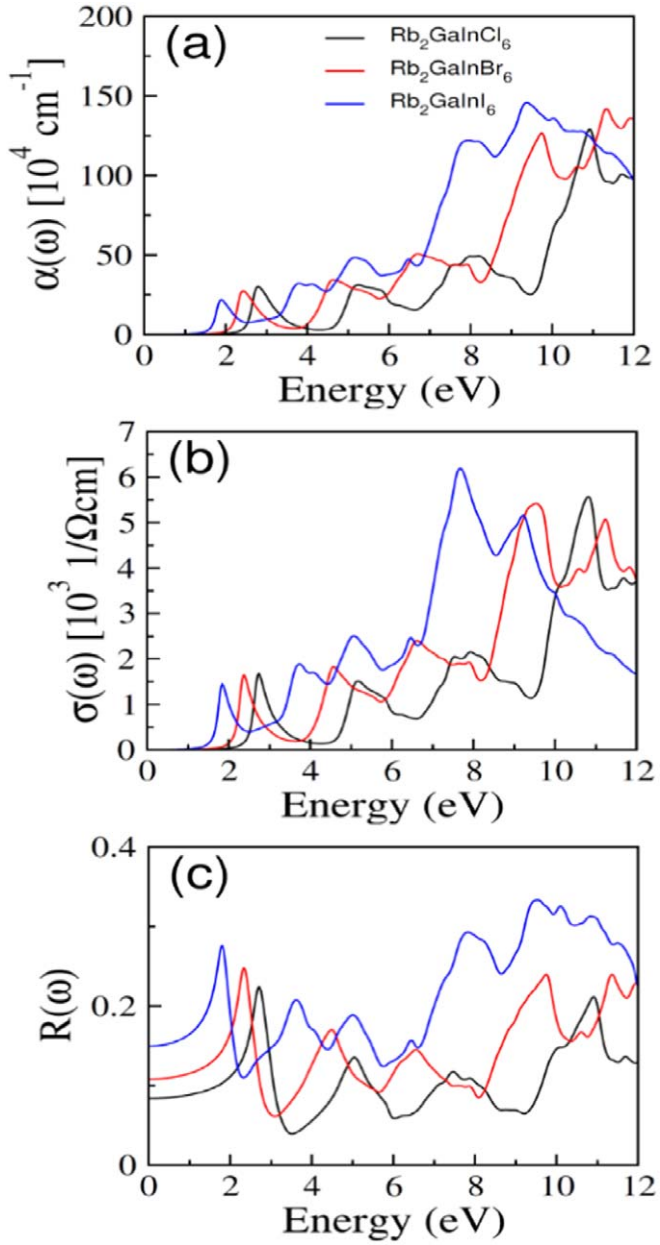

Figure 7. Calculated values of $\alpha(\omega)$, $\sigma(\omega)$ and $R(\omega)$ of Rb_2GaInX_6 (X = Cl, Br, I) by using mBJ-potential.

Table 3. Estimated values at 300K of Electrical conductivity (σ/τ), Thermal conductivity (k_e/τ), Seebeck parameter (S), Power factor (PF), and figure of merit through mBJ-potential for the structure of Rb_2GaInX_6 (X = Cl, Br, I).

Perovskites	$\sigma/\tau(\times 10^{18}/\Omega ms^{-1})$	$k_e/\tau(\times 10^{14}Wm^{-1}K^{-1})$	S (μVK^{-1})	PF ($\times 10^{10}$ W mK^{-2}s^{-1})	ZT
$Rb_2GaInCl_6$	6.51	1.08	197.25	2.53	0.72
$Rb_2GaInBr_6$	5.74	0.92	203.03	2.36	0.74
Rb_2GaInI_6	2.63	0.62	248.66	1.62	0.76

The heat frow per unit area of the material when a temperature gradient is maintaine across its terminal is termed as the thermal conductivity (k/τ). The thermal conductivity possesses two parts: the phonon part (k_{ph}) and the electronic part (k_e). Nevertheless, in the present work, only the electronic part is discussed because the contribution of phonons is not in notice at low temperature, and the BoltzTrap code restricts it. It can be observed from figure 8(c) that the value of k_e/τ rises with an increase in temperature. Because of the larger ionic radii, the thermal collision increases [23].

The calculated values of k_e/τ are 1.08/0.920/0.62 $\times$ 10^{14}W mK^{-1} for the material Rb_2GaInX_6 (X = Cl, Br, I), respectively. It can be noticed that explored materials have a low value of k_e/τ.So, it is a suitable applicant for

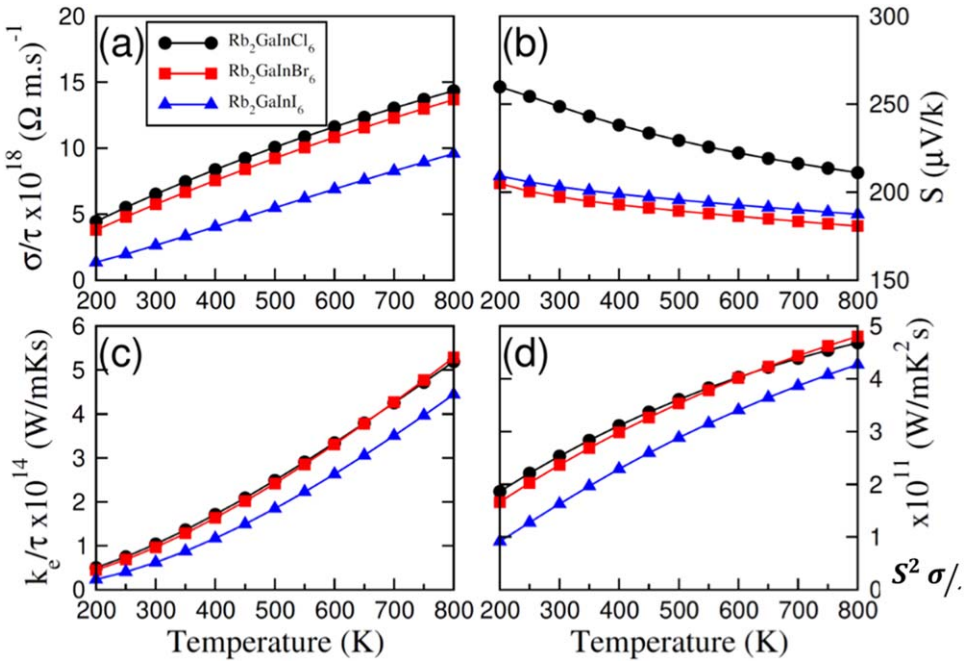

Figure 8. Estimated values of (a) (σ/τ), (b) (k_e/τ), (c) (S) and (d) (PF) for Rb_2GaInX_6 (X = Cl, Br, I).

thermoelectric device fabrication. The thermal conductivity can be determined by the formula [14].

$$k^{e}_{a\beta(T,\mu)} = \frac{1}{e^2T\Omega}\int \sigma_{a\beta}(\varepsilon)(\varepsilon - \mu)\left[-\frac{\partial f0(T,\varepsilon,\mu)}{\partial\mu}\right]d \tag{10}$$

The capability of a material to produce electrothermal voltage when a temperature difference exists between the ends of a material is called Seebeck coefficient. It is usually measured in μVK^{-1}. It can be noticed from the graph that there is a reduction in the value of S with the temperature rise. This observed behavior confirms the conduction of small polarons in the material with charge carriers independent of temperature [24]. The decreasing behavior is due to the increasing thermal movement of carriers with decreasing value of Seebeck voltage. The obtained positive value of the Seebeck coefficient predicts the flow of positive charge carriers and vice versa for negative values. The Seebeck coefficient can be calculated by using the formula.

$$S_{\alpha\beta(T,\mu)} = \frac{1}{eT\Omega\sigma_{a\beta}(T,\mu)}\int \sigma_{a\beta}(\varepsilon)(\varepsilon - \mu)\left[-\frac{\partial f0(T,\varepsilon,\mu)}{\partial\varepsilon}\right] \tag{11}$$

The calculated values of the Seebeck coefficient for Rb_2GaInX_6 (X = Cl, Br, I) are 197.25/203.03/248.66 μVK^{-1}, respectively in the temperature range of (200–800K).

Power factor (PF) is the percentage expression of energy efficiency of a thermoelectric device. It shows the overall efficient performance of the double perovskite materials for energy conservation devices. The following equation can represent it:

$$PF = \frac{S^2\sigma}{\tau} \tag{12}$$

Figure 8(d) shows that the power factor increases when there is a rise in temperature because it is directly related to the value of S and σ. The estimated value of PF at room temperature is higher for Cl(2.53×10^{10} W $mK^{-2}s^{-1}$) than other compositions.

The value of the figure of merit indicates the effective functioning of thermoelectric (TE) devices. For a perfect thermoelectric device, the value of ZT must be equal to or greater than unity. The below relation can calculate the figure of merit:

$$ZT = \frac{\sigma TS^2}{k} \tag{13}$$

S denotes the Seebeck coefficient, σ and k represent the electrical and thermal conductivities, respectively.

It can be noted from figure 9 that the value of ZT decreases as the Temperature (K) increases. As observed at high temperatures, the bandgap value reduces, so the value of ZT is also reduced [25]. The noted value of ZT is 0.72 at 800K for $Rb_2GaInCl_6$, and similarly, for other compositions, values are given in table 3. Since external

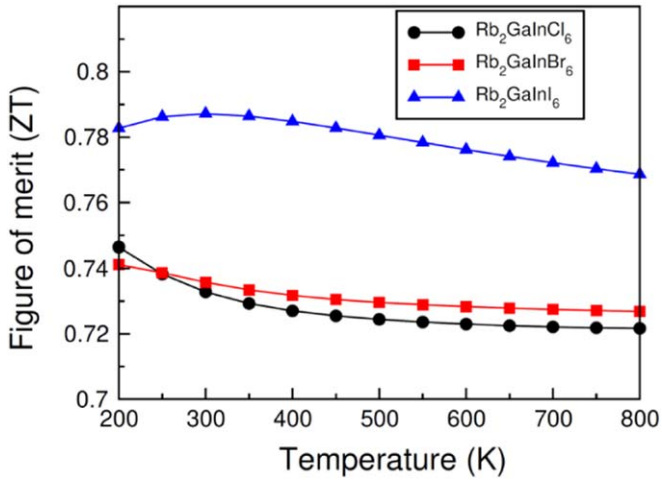

Figure 9. The calculated figure of merit (ZT) for Rb_2GaInX_6 (X = Cl, Br, I).

pressure helps mold electronic properties, which ultimately affect optical and thermal transports of materials [26, 27], similar strategies could also be practiced for the materials under investigation to make them sound as per technological requirements.

4. Conclusion

In summary, by using mBJ potential for the first time, the optoelectronic and thermoelectric properties of Rb_2GaInX_6 (X = Cl, Br, I)halide perovskite has been completely investigated based on the first principles study. The estimated structural parameters truly satisfy the experimental results. The calculated Paugh's value, which is larger than 1.75 ofRb_2GaInX_6 (X = Cl, Br, I), predicts the ductile nature of the materials.The obtained results of bandgap structure reveals that all the three materials own indirect bandgaps of2.20eV ($Rb_2GaInCl_6$),1.55eV ($Rb_2GaInBr_6$) and 0.90eV (Rb_2GaInI_6). The high value of absorption $\alpha(\omega)$ parameter in the UV and visible region within energy range (2–8eV) proves that explored materials are potential candidates for optical devices. Furthermore, the obtained value of ZT for $Rb_2GaInCl_6$is ~0.73 at room temperature makes it useful for thermoelectric applications.

Acknowledgments

Dr R Neffati extend his appreciation to the Deanship of Scientific Research at King Khalid University for financial support through research groups program under grant number (R.G.P. 1/139/43).

Data availability statement

All data that support the findings of this study are included within the article (and any supplementary files).

ORCID iDs

N A Noor https://orcid.org/0000-0001-8039-1424

References

[1] Ismail B I and Ahmed W H 2009 Thermoelectric power generation using waste-heat energy as an alternative green technology.recent patents on electrical & electronic engineering (formerly recent patents on *Electrical Engineering)* **2** 27–39
[2] Kangsabanik J, Sugathan V, Yadav A, Yella A and Alam A 2018 Double perovskites overtaking the single perovskites: A set of new solar harvesting materials with much higher stability and efficiency *Phys. Rev. Mater.* **2** 055401
[3] Flemban T H, Zelai T, Mahmood Q, Devi A A S, Sajjad M, Alhossainy M H, Somaily H H, Mera A, Alharthi S and Amin M A 2022 Half-metallic ferromagnetism and thermoelectric properties of double perovskites $Rb_2Z(Cl/Br)_6$ (Z = Ta, W, Re) *J. Alloys and Compounds* **894** 162313
[4] Maiti T, Saxena M and Roy P 2018 Double perovskite (Sr_2 B′B″O_6) oxides for high-temperature thermoelectric power generation—a review *J. Mater. Res.* **34** 107–25

[5] Noor N A, Iqbal M W, Zelai T, Mahmood A, Shaikh H M, Ramay S M and Al-Masry W 2021 Analysis of direct band gap A_2ScInI_6 (A = Rb, Cs) double perovskite halides using dft approach for renewable energy devices *J. Mater. Res.* **13** 2491–500
[6] Faizan M, Murtaza G, Khan S H, Khan A, Mehmood A, Khenata R and Hussain S 2016 First-principles study of the double perovskites Sr_2XOsO_6 (X = Li, Na, Ca) for spintronics applications *Bull. Mater. Sci.* **39** 1419–25
[7] Parrey K A, Khandy S A, Islam I, Laref A, Gupta D C, Niazi A and Rubab S 2018 Electronic structure, optical and transport properties of double perovskite La_2NbMnO_6: a theoretical understanding from DFT calculations *J. Electron. Mater.* **47** 3615–21
[8] Ullah R, Ali M A, Murtaza G, Khan A and Mahmood A 2020 *Ab initio* study for the structural, electronic, magnetic, optical, and thermoelectric properties of K_2OsX_6 (X = Cl, Br) compounds *Int. J. Energy Res.* **44** 9035–49
[9] Nabi M, Bhat T M and Gupta D C 2019 Effect of pressure on electronic, magnetic, thermodynamic, and thermoelectric properties of tantalum-based double perovskites Ba_2MTaO_6 (M = Mn, Cr) *Int. J. Energy Res.* **43** 4229–42
[10] Razzaq M A and Islam T 2020 Structural, mechanical and optoelectronic study of double perovskite Cs_2SnBr_6 using first principles calculation *G.J.M.S.E.* **125** 6–9
[11] Dar S A, Sharma R, Srivastava V and Sakalle U K 2019 Investigation on the electronic structure, optical, elastic, mechanical, thermodynamic and thermoelectric properties of wide band gap semiconductor double perovskite Ba_2InTaO_6 *RSC Adv.* **9** 9522–32
[12] Blaha P, Schwarz K, Madsen G, Kvasnicka D and Luitz J 2002 *WIEN2k, AnAugmented Plane Wave Plus Local Orbitals Program for Calculating CrystalProperties* (Austria: Vienna University of Technology) 2001
[13] Haid S, Benstaali W, Abbad A, Bouadjemi B, Bentata S and Aziz Z 2019 Thermoelectric, structural, optoelectronic and magnetic properties of double perovskite Sr_2CrTaO_6: First principle study *M.S.E.B* **245** 68–74
[14] Sahnoun O, Bouhani-Benziane H, Sahnoun M and Driz M 2017 Magnetic and thermoelectric properties of ordered double perovskite Ba_2FeMoO_6 *J. Alloys Compd.* **714** 704–8
[15] Tyuterev V G and Vast N 2006 Murnaghan's equation of state for the electronic ground state energy *Comput. Mater. Sci.* **38** 350–3
[16] Tariq M, Ali M A, Laref A and Murtaza G 2020 Anion replacement effect on the physical properties of metal halide double perovskites Cs_2AgInX_6 (X = F, Cl, Br, I) *Solid State Commun.* **314** 113929
[17] Razzaq M A and Islam M M 2019 Investigation of structural, elastic, electronic and optical properties of ternary KLiTe: a first principles study *I.R.J.E.T.* **06** 2395–0072
[18] Mahmood Q, Younas M, Ashiq M G B, Ramay S M, Mahmood A and Ghaithan H M 2021 First principle study of lead-free double perovskites halides Rb_2Pd $(Cl/Br)_6$ for solar cells and renewable energy devices: a quantum DFT *Int. J. Energy Res.* **45** 14995–5004
[19] Ray R, Himanshu A K, Lahiri J, Kumar U, Sen P, Bandyopadhyay S K and Sinha T P 2016 Optical and electronic properties of double perovskite Ba_2ScSbO_6 *AIP Conf. Proc.* 1731 (United States : Publishing LLC) 140041AIP
[20] Al-Lehyani I H 2021 A first-principle study of the stability and electronic properties of halide inorganicdouble perovskite Cs_2PbX_6 (X = Cl, I) for solar cell application *Arab. J. Chem.* **14** 102920
[21] Bhamu K C, Soni A and Sahariya J 2018 Revealing optoelectronic and transport properties of potential perovskites Cs_2PdX_6 (X = Cl, Br): a probe from density functional theory (DFT) *Sol.Energy* **162** 336–43
[22] Guechi N, Bouhemadou A, Bin-Omran S, Bourzami A and Louail L 2018 Elastic, optoelectronic and thermoelectric properties of the lead-free halide semiconductors Cs_2AgBiX_6 (X = Cl, Br): *ab initio* investigation *J. Electron. Mater.* **47** 1533–45
[23] Siad A B, Baira M and Siad M B 2021 Structural, mechanical, optoelectronic and thermoelectric properties of double perovskite compounds Cs_2TeX_6 (X = Br, I) for energy storage applications: First *principles investigations, J. Phys. Chem. Solids* **152** 109955
[24] Mahmood Q, Hassan M, Flemban T H, Haq B U, AlFaify S, Kattan N A and Laref A 2021 Optoelectronic and thermoelectric properties of double perovskite Rb2PtX6 (X = Cl, Br) for energy harvesting: first-principles investigations *J. Phys. Chem. Solids* **148** 109665
[25] Buch J J U, Pathak T K, Lakhani V K, Vasoya N H and Modi K B 2007 High temperature thermoelectric power study on calcium substituted lanthanum manganites *J. Phys. D: Appl. Phys.* **40** 5306
[26] Nazir S, Mahmood I, Noor N A, Laref A and Sajjad M 2019 Ab-initio simulations of $MgTiO_3$ oxide at different pressure *High Energy Density Phys.* **33** 100715
[27] Aslam M, Khan A, Hashmi M A, Sajjad M, Algrafy E, Mustafa G M, Mahmood A and Ramay S M 2020 Physical characteristics of $CdZrO_3$ perovskite at different pressure for optoelectronic application *J Mater. Res. Technol.* **9** 9965